International Journal of Engineering and Advanced Technology (IJEAT)
ISSN: 2249-8958 (Online), Volume-2 Issue-6, August 2013

Anatomizing Quantum Transport in Molecular Junctions with Cyanide and its Isomer as Anchors

Rupan Preet Kaur, Ravinder Singh Sawhney, Harpinder Kaur

Abstract: ***The electrical properties of SAMs on gold surface with different alligator clips at each ends were explored for an anthracene molecule. We probed charge transport characteristics of anthracene with two different anchor groups- Cyanide and its isomer Isocyanide attached to anthracene at each side and sandwiched between two gold electrodes. Through I-V Curves, conductance-voltage curves, differential conductance-voltage curves and transmission spectrum, we found that anthracene-cyanol-isocyanol (ACI) exhibited highest current, conductance and transmissions whereas anthracenedisocyanol (ADC) exhibited least current, conductance and transmissions. This highest conduction of ACI was on account of very strong bonding between gold electrodes and corresponding –CN anchor group whereas lowest conduction of ADC was because of weaker bonding between gold electrodes and –NC anchor group. The conduction exhibited by gold-CN bond and gold-S bond was found to be similar hence concluding that both these bonds (Au-CN and Au-S) have approximately similar strength.***

Index Terms: Nanoscale, Alligator Clips, HOMO, LUMO, Isomer.

I. INTRODUCTION

Understanding electron transport through nanoscale junctions or molecular devices connected to metallic electrodes may be the basis of future molecular electronics technology. It is a great challenge to achieve electronically transparent connections between metal electrodes and organic molecules [1], so as to minimize resistances introduced by the chemical linkers normally used to form such interfaces [2]. Experimental and theoretical studies of single-molecule transport have focused considerable efforts on molecules, with the hope that versatile electronic devices can be engineered from these building blocks. One area in which there has been extensive work with Huckel models, [3-22] as well as recent calculations with more realistic approaches, [23–25] is the prediction of systems where quantum-interference effects dominate the molecular transport. The numerous experimental results so far have concluded that the charge transport through molecular junctions [26, 27] is controlled by the intrinsic properties of the molecules, the contacts (“alligator clips”), and the metal leads. These include the molecular length, conformation, the gap between HOMO and LUMO, the alignment of this gap to the metal Fermi level, temperature, mechanical stress and the metal-molecule coordination geometry.

Manuscript published on 30 August 2013.
***** Correspondence Author (s)
Rupan Preet Kaur, Department of Electronics Technology, Guru Nanak Dev University, Amritsar, India.
Ravinder Singh Sawhney, Department of Electronics Technology, Guru Nanak Dev University, Amritsar, India.
Harpinder Kaur, Department of Electronics Technology, Guru Nanak Dev University, Amritsar, India.

In the previous research, we observed the effect of changing anchor groups on the electron transport characteristics of Anthracene molecule bridged between two gold electrodes and concluded the best suitability of thiol group. We further extended our research by having different anchor groups at each side of anthracene molecule and observed variable quantum behaviour. Through various research studies, the scientists and scholars have always emphasised the use of thiol group as anchor, as it ensures the strong chemical bonding to the leads with the current flow mainly modulated by the molecular HOMO level. A strong metal-molecule bond and a smaller energy difference are essential for the molecular junction to show high conductance. The energy of the molecular orbital varies with the end group of the molecule [28]. It is important to develop new end groups other than a thiol to enable more stable and higher conductance single molecular junctions. In this research work, we have investigated the use of Cyanide and its isomer- Isocyanide as anchor groups with anthracene molecule sandwiched between two gold electrodes. Different geometries were constructed by having once cyanide group and isocyanide group at two different sides of anthracene, then reversed their positions giving Anthracene-isocynaol-cyanol(AIC) and anthracene-cyanol-isocyanol (ACI). In third epoch, we considered cyanol group and thiol group giving it name- Anthracene thiol-cyanol (ATC) and lastly isocyanol group was placed at either side of anthracene i.e. Anthracene di-isocyanol(ADC). Their charge transport characteristics were computed and reported as below.

II. MODELING & SIMULATION

We have considered our modelling and simulation of the electron transport through anthracene stringed to two semi-infinite gold electrodes having [111] configuration using two different anchor groups- Cyanide and Isocyanide at each side. For our modelling, we employed semi-empirical extended huckel theory (EHT) for the purpose of tight binding as well as time constraint. The resultant molecular junctions formed are shown in figure 1 which shows anthracene molecule stretched between two gold electrodes with varied positions of cyanide, isocyanide and thiol groups. In first epoch, we had isocyanide bounding anthracene to left electrodes and cyanide connecting anthracene to right gold electrodes. Both anchor positions were reversed in second epoch. In third epoch, thiol group bonded anthracene to left electrodes and isocyanide group to the right electrodes. Lastly, we considered isocyanide at either sides of anthracene connecting the gold electrodes. These ‘alligator clips’ or anchor groups connected anthracene to electrodes via para positions as para positions are linearly conjugated, whereas the meta position is cross-conjugated [29].

Published By:
Blue Eyes Intelligence Engineering and Sciences Publication (BEIESP)

Gold electrodes have been generally used in single molecule junctions because of their stability in air. The quantum mechanical First-principle transport calculations for a two-probe system were performed using Atomistic Tool Kit 12.2.0 [30] and its graphical interface employing semi-empirical Extended Huckel Device Theory. The aim of this work is to compute the charge transport characteristics of AIC, ACI, ATC and ADC and to conclude the most optimum anchor group pair for anthracene molecule. The bias voltage was varied from -1.2V to 1.2V with step size of

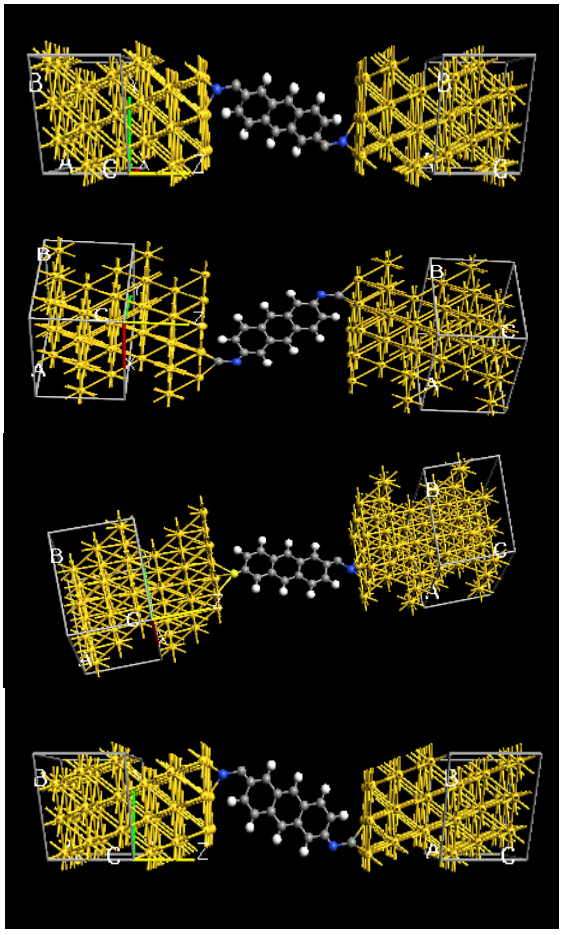

Figure 1: a) AIC b) ACI c) ATC d) ADC stringed to two gold electrodes at para positions

0.4V and the corresponding I-V curve, transmission spectra and conductance values were simulated, reported and their graphical interpretation was highlighted.

III. RESULTS & DISCUSSIONS

We have modelled anthracene molecule with different end group anchors- Cyanide and Isocyanide sandwiched between two semi-infinite gold electrodes (1, 1, 1) orientation. We simulated I-V curves, transmission spectra and conductance curves at various applied bias ranging from -1.2V to 1.2V.

A. I-V Curves

The current can be calculated by firstly calculating transmission function given by [31]:

$$T(E,V) = 1/\Omega \int_{\Omega} dK\, T^{k}(E,V) \quad (1)$$

The transmission function at k,, $T^{k}(E)$ are expressed in terms of Green's functions as [26,27]:

$$T^{k}(E,V)=Tr\,[\Gamma_1^{k}(E,V)\, G_M^{k}(E,V)\, \Gamma_2^{k}(E,V)\, G_M^{k'}(E,V)] \quad (2)$$

Expression (2) describes the broadening of molecular energy levels due to the coupling to electrodes. Then I-V characteristics can be computed by Landauer - Buttiker formulism [32] given by:

$$I(V)=2e/h.\int T(E)[f(E-\mu_s)-f(E-\mu_D)]De \quad (3)$$

The values of currents at different bias voltages from -1.2 to 1.2V were computed through the simulations that are reported in table 1 and shown in figure 2.

Table 1: Current (nA) versus voltage (v)

Bias voltage(v)	AIC	ACI	ATC	ADC
-1.2	-393	-817	-5816	-1710
-0.8	-30	-501	-2804	-1717
-0.4	-20	-257	-518	-166.5
0	0	0	0	0
0.4	1720	563	940	26
0.8	2207	10644	3792	91.5
1.2	2400	11918	4576	984

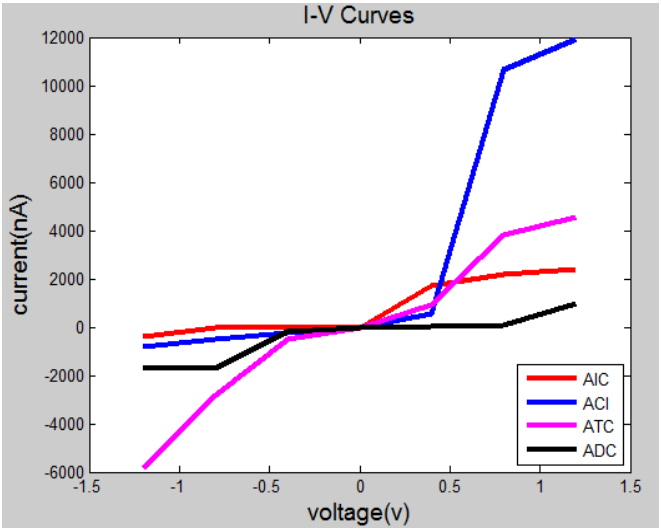

Figure 2: Current versus Voltage

From figure 2 and table 1, we observed that with increase in bias voltage, current increased correspondingly. ACI exhibited highest current followed by ATC, further followed by AIC and ADC exhibited least current. We found that by switching the anchor positions i.e. AIC to ACI, prominent increase in current from 2.4µA to 10.6 µA was observed. This varied current behaviour was on account of different bond strength between the cyanide and isocyanide group with the gold electrodes. The strength of the metal-CN bond is comparable to that of the metal-S bond. Because of this effective interaction between the isocyanide group and metals, air stable isocyanide SAM films are formed on Au [33], as with the case of thiol SAMs [34]. This strong Au-CN bond may contribute to increase in the conductance of the junction whereas.

Published By:
Blue Eyes Intelligence Engineering and Sciences Publication (BEIESP)

Au-NC bond is weaker than that of Au-S and Au-CN bond. Theoretical calculations shows that the conductance of the molecular junction with the metal-NC bond is three times smaller than that with the metal-S bond [35, 36]. ACI and ATC high current was on account of this strong metal-group bond. ACI exhibited more current than ATC as in ACI, there were Au-CN bonds at either side of anthracene molecule, hence contributing to high conduction and high current whereas in ATC, there was Au-S bond at one side and Au-NC bond at other leading to comparatively low conduction. AIC and ADC exhibited lower current on account of the weaker bonding between gold and –NC group.

B. Conductance

The quantized conductance of the molecule can be given by the relation:

$$G_0 = N e^2 / h \quad (4)$$

Here e and h are electron charge and plank's constant respectively, while N depends upon the spin. The quantized conductance G_0 is the conductance at zero bias and this value works out to be 77.5 µS. The total transmission coefficient is also a function of conductance at any bias voltage and is given by:

$$G = G_0 T(E_F) \quad (5)$$

where $T(E_F)$ is the transmission coefficient at Fermi energy. The conductance values of ATS were computed corresponding to the bias voltages and reported as shown in table 2 and plotted in figure 3.

Table2: Conductance (µS) versus voltage (v)

Bias voltage(v)	AIC	ACI	ATC	ADC
-1.2	0.24	0.83	1.13	0.004
-0.8	0.10	0.72	9.2	0.006
-0.4	0.01	0.68	1.46	1.76
0	0.142	0.78	1.35	0.007
0.4	1.57	1.77	2.98	0.009
0.8	0.204	9.1	2.75	0.121
1.2	0.64	0.58	1.45	8.4

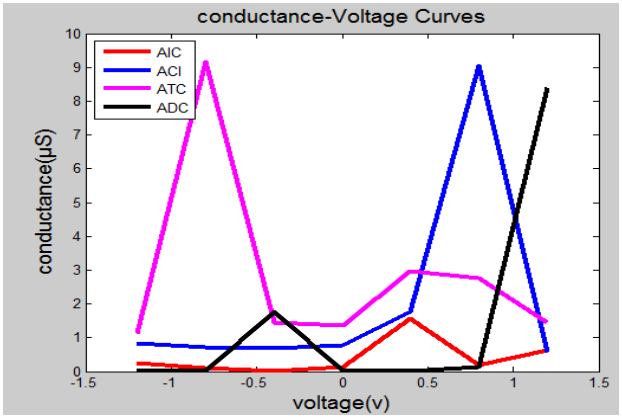

Figure 3: Conductance versus voltage

From table 2 and figure 3, we observed different peaks exhibited by AIC, ACI, ATC and ADC. AIC and ADC exhibited lower conductance but ADC exhibited highest conductance at 1.2V i.e. 8.4µS. The low conductance of AIC and ADC proves the weak bonding of -NC with gold electrodes but high conductance of approx. $0.11G_0$ of ADC at high bias can be attributed to the degradation in the energy gap between Fermi level of gold electrodes and HOMO level of ADC with increasing positive bias. ATC exhibited higher conductance during negative bias region whereas lower conductance during positive bias. Its maxima was reported as 9.2 µS ~0.12 G_0 at -0.8V whereas ACI showed contrasting behaviour i.e. conductance was more during positive bias and lesser during negative bias. The maximum conductance reported by ACI was 9.1 µS almost same as that of ATC but at +0.8V. Isocyanide(-NC) binds to the metal via a strong coordination bond by effective donation to metal and back donation from metals because of which its conduction was found to be maximum. High conductance at low bias and low conductance with increasing bias in ATC was on account of increasing mis-alignment in the energy gap between Fermi level of gold and ATC at high bias voltages. This behaviour was further investigated in differential conductance behaviour.

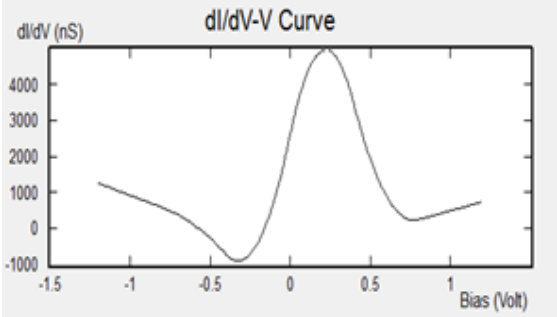

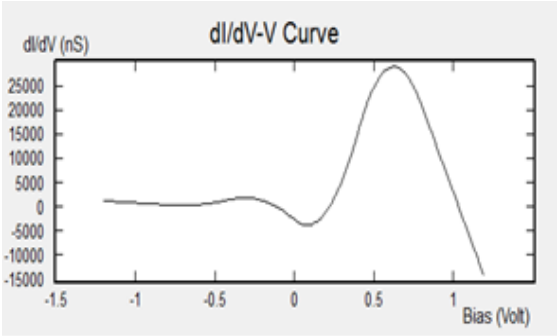

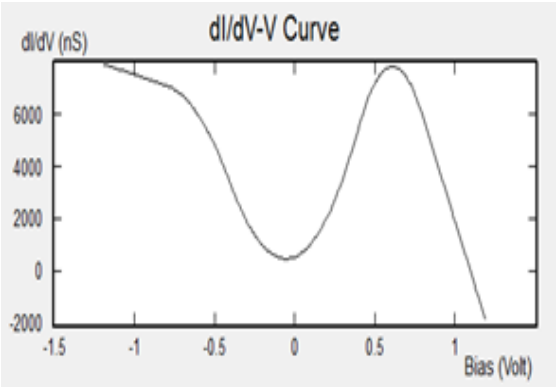

Published By:
Blue Eyes Intelligence Engineering
and Sciences Publication (BEIESP)

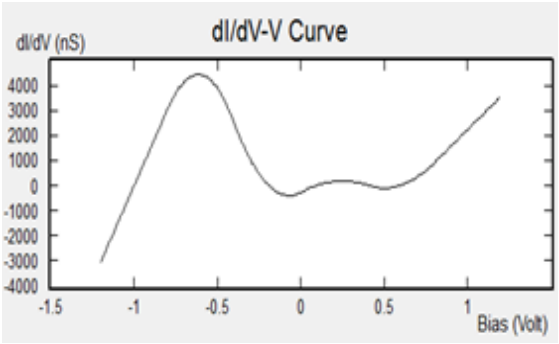

Figure 4: dIdV-V curves of a) AIC b) ACI c) ATC d) ADC

IV. TRANSMISSION SPECTRUM

The transmission spectrum shows the coupling between the electrodes and the molecule that leads to overlapping of the hybridized orbitals and a change in HOMO-LUMO gaps. The stronger the coupling, more the orbitals are broadened and lesser will be the energy gap to jump for electrons. Sharp peaks in the spectrum show maximum transmissions (smaller HOM-LUMO gap) whereas flatness shows minimum transmissions (greater HOM-LUMO gap). Figure 5 shows the transmission spectrum of the different geometries under study. The spectrum with maximum transmissions in figure 5b) shows the reason why ACI molecule exhibited highest conduction. Since the spectrum shows the peaks throughout the bias region from -5V to 5V, it indicates the smallest HOMO- LUMO gap exhibited by ACI.AIC was found to be having second large number of transmissions as shown in figure 5a).

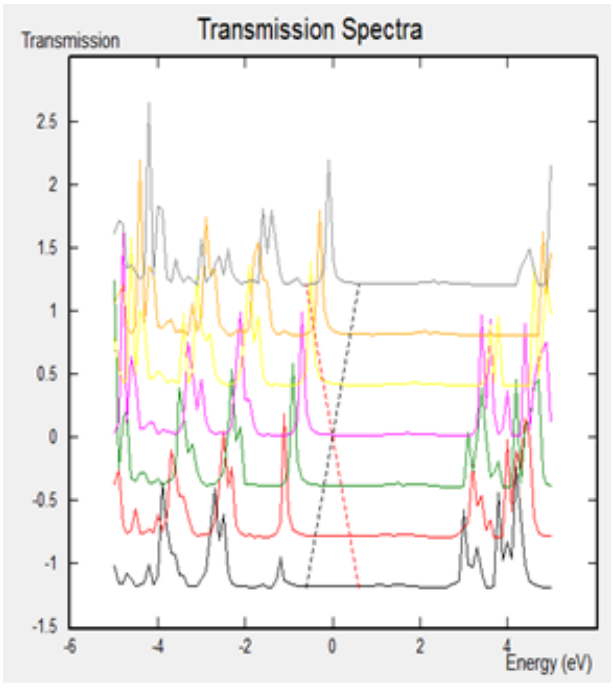

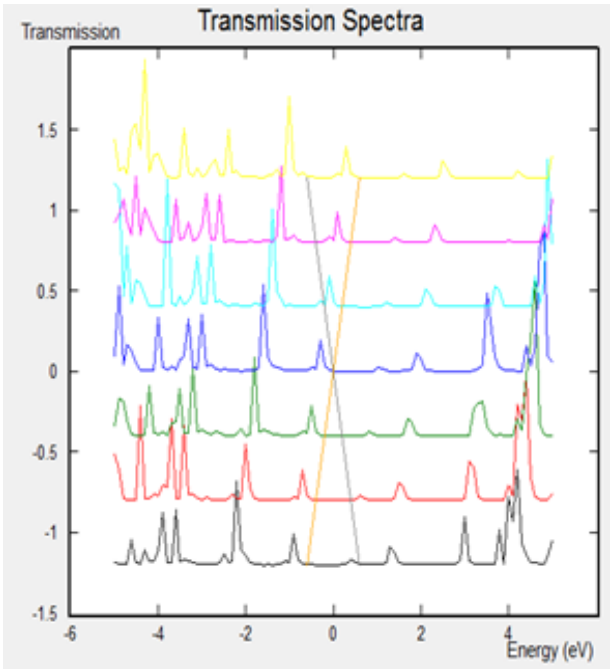

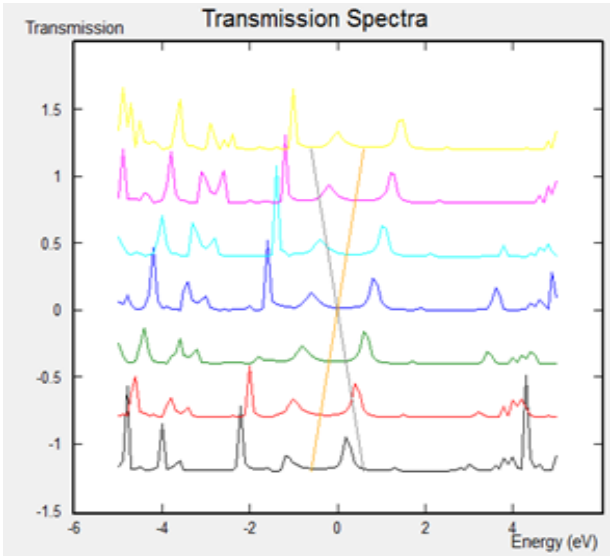

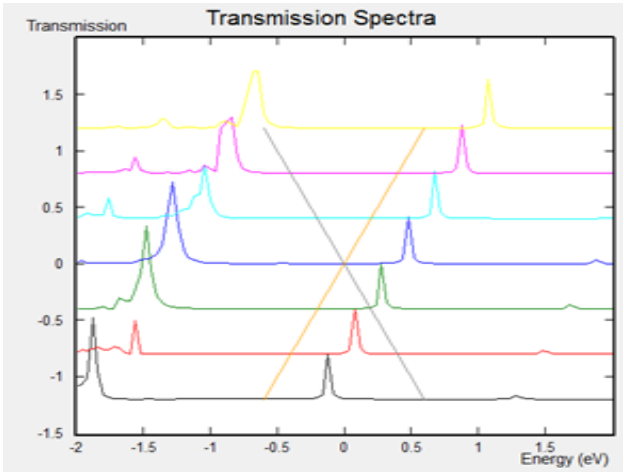

Figure 5: Transmission Spectrum of a) AIC b)ACI c) ATC d) ADC)

Published By:
Blue Eyes Intelligence Engineering
and Sciences Publication (BEIESP)

Hence, electrons need to gain small energy to cross the smaller gap and hence contribute in high conduction. Figure 5c) and d) shows transmission spectrum of ATC and ADC. ADC exhibited least transmissions and its whole spectrum showed flatness during the entire energy range. ATC exhibited more transmissions and comparatively lesser flatness in the spectrum. Hence, we can say that the maximum energy gap was found in ADC followed by ATC and further followed by AIC whereas ACI exhibited smallest energy gap. The increasing order of transmissions exhibited by these molecules was found as: ADC < ATC < AIC < ACI.

V. CONCLUSIONS

The charge transport parameters of anthracene with different anchor groups(-CN,-NC,-S) were performed and different characteristics were simulated from which we concluded that because of high strength of Au-CN bond and weaker Au-NC bond, ACI supported highest conduction whereas ADC supported least conduction. The increasing order of charge transport was concluded as: ADC < ATC < AIC < ACI. The results produced through this simulation work are reproducible and can be further extended to observe the effect of two different contacts on the conduction of molecular devices. This can be further extended by considering various other anchors like -COOH, - NH_2 groups and their transport characteristics can be compared and the most optimal pair of alligator clips can be concluded for highest possible conduction of molecular devices where we can use anthracene molecule for design of molecular electronic devices such as organic solar cells, OLED (organic light emitting diodes) and OTFT (organic thin film transistor).

ACKNOWLEDGMENT

The authors acknowledge the support by C.S.I.R. under Grant No. 22(0519)10/EMR-II.

REFERENCES

1. (a) Nitzan, A.; Ratner, M. A., *Science* **2003,** 300, (5624), 1384-1389; (b) Joachim, C.; Ratner, M. A., *PNAS* **2005,** 102, (25), 8801-8808.
2. (a) Venkataraman, L.; Klare, J. E.; Tam, I. W.; Nuckolls, C.; Hybertsen, M. S.; Steigerwald, M. L., *Nano Lett.* **2006,** 6, (3), 458 - 462; (b) Chen, F.; Li, X. L.; Hihath, J.; Huang, Z. F.; Tao, N. J., *J. Am. Chem. Soc.* **2006,** 128, (49), 15874- 15881; (c) Park, Y. S.; Whalley, A. C.; Kamenetska, M.; Steigerwald, M. L.; Hybertsen, M. S.; Nuckolls, C.; Venkataraman, L., *J. Am. Chem. Soc.* **2007,** 129, (51), 15768-15769; (d) Kiguchi, M.; Tal, O.; Wohlthat, S.; Pauly, F.; Krieger, M.; Djukic, D.; Cuevas, J. C.; van Ruitenbeek, J. M., *Phys. Rev. Lett.* **2008,** 101, (4), 046801; (e) Martin, C. A.; Ding, D.; Sorensen, J. K.; Bjornholm, T.; van Ruitenbeek, J. M.; van der Zantt, H. S. J., *J. Am. Chem. Soc.* **2008,** 130, (40), 13198-13199; (f) Schneebeli, S. T.; Kamenetska, M.; Cheng, Z.; Skouta, R.; Friesner, R. A.; Venkataraman, L.; Breslow, R., *J. Am. Chem. Soc.* **2011,** 133, (7), 2136-2139; (g)Mishchenko, A.; Zotti, L. A.; Vonlanthen, D.; Burkle, M.; Pauly, F.; Cuevas, J. C.; Mayor, M.; Wandlowski, T., *J. Am. Chem. Soc.* **2011,** 133, (2), 184-187; (h) Kosov, D. S.; Li, Z. Y., *J. Phys. Chem. B* **2006,** 110, (20), 9893-9898; (i) von Wrochem, F.; Gao, D. Q.; Scholz, F.; Nothofer, H. G.; Nelles, G.; Wessels, J. M., *Nat. Nano.* **2010,** 5, (8), 618-624.
3. P. Sautet, C. Joachim, Chem. Phys. Lett. 1988 153,511.
4. P. Sautet, C. Joachim, Chem. Phys. 1989, 135, 99.
5. C. Patoux, C. Coudret, J. P. Launay, C. Joachim, A. Gourdon, Inorg. Chem. 1997, 36, 5037.
6. C. Joachim, J. K. Gimzewski, H. Tang, Phys. Rev. B 1998, 58, 16407.
7. E. G. Emberly, G. Kirczenow, J. Phys. Condens. Matter 1999, 11, 6911.
8. T. S. Elicker, J. S. Binette, D. G. Evans, J. Phys. Chem. B 2001, 105, 370.
9. R. Baer, D. Neuhauser, J. Am. Chem. Soc. 2002, 124, 4200.
10. S. N. Yaliraki, M. A. Ratner, Ann. N. Y. Acad. Sci. 2002, 960, 153.
11. C. Kalyanaraman, D. G. Evans, Nano Lett. 2002, 2, 437.
12. R. Collepardo-Guevara, D. Walter, D. Neuhauser, R. Baer, Chem. Phys. Lett. 2004, 393, 367.
13. M. H. van der Veen, M. T. Rispens, H. T. Jonkman, J. C. Hummelen, Adv. Funct. Mater. 2004, 14, 215.
14. K. Walczak, Cent. Eur. J. Chem. 2004, 2, 524.
15. D. Walter, D. Neuhauser, R. Baer, Chem. Phys. 2004, 299, 139.
16. F. Zhai, H. Q. Xu, Phys. Rev. B 2005, 72, 195 346.
17. M. Ernzerhof, M. Zhuang, P. Rocheleau, J. Chem. Phys. 2005, 123, 134704.
18. D. M. Cardamone, C. A. Stafford, S. Mazumdar, Nano Lett. 2006, 6, 2422.
19. M. Ernzerhof, H. Bahmann, F. Goyer, M. Zhuang, P. Rocheleau, J. Chem. Theory Comput. 2006, 2, 1291.
20. F. Goyer, M. Ernzerhof, M. Zhuang, J. Chem. Phys. 2007, 126, 144 104.
21. S. K. Maiti, Phys. Lett. A 2007, 366, 114.
22. G. C. Solomon, D. Q. Andrews, T. Hansen, R. H. Goldsmith, M. R. Wasielewski,R. P. Van Duyne, M. A. Ratner, J. Chem. Phys. 2008, 129, 054701.
23. S.-H. Ke, W. Yang, H. U. Baranger, Nano Lett. 2008, 8, 3257.
24. G. C. Solomon, D. Q. Andrews, R. P. Van Duyne, M. A. Ratner, J. Am. Chem. Soc. 2008, 130, 7788.
25. D. Q. Andrews, G. C. Solomon, R. H. Goldsmith, T. Hansen, M. R. Wasielewski, R. P. V. Duyne, M. A. Ratner, J. Phys. Chem. C 2008, 112, 16991.
26. Nitzan, A.; Ratner, M. A. *Science* **2003**, *300* (5624), 1384–1389.
27. Pecchia, A.; Di Carlo, A. *Rep. Prog. Phys.* **2004**, *67* (8), 1497–1561.
28. Manabu Kiguchi, Shinichi Miura, Kenji Hara, Masaya Sawamura, Kei Murakoshi, Conductance of a single molecule anchored by an isocyanide substituent to gold electrodes, Division of Chemistry, Sapporo, 060-0810, Japan(2008).
29. Ravinder Singh Sawhney, Derick Engles, Geometry Related Quantum Interference for Stress and Conductance of an Organic Molecule, *Conf. Proceedings Nanocon 2012, BVU, pp.1219-1224*.
30. Atomistic Toolkit Manual, Quantumwise Inc.
31. Yong-Hoon Kim ,Seung Soon Jang and William A. Goddard, Conformations and charge transport characteristics of biphenyldithiol self-assembled-monolayer molecular electronic devices: A multiscale computational study, *The Journal of Chemical Physics* 122, 244703 (2005).
32. S. Datta, Electronic Transport in Mesoscopic Systems (*Cambridge University Press, Cambridge, UK*, 1995).
33. D.L. DuBose, R.E. Robinson, T.C. Holovics, D.R.Moody, E. C. Weintrob, C.L. Berrie, and M.V. Barybin, Langmuir 22, 4599 (2006).
34. K. Hara, K. Iwahashi, Y. Kanamori, S. Naito, S. Takakusagi, K. Uosaki, and M. Sawamura, Chem. Lett.35, 870 (2006).
35. N. D. Lang and Ph. Avouris, Phys. Rev. B 64, 125323 (2001).
36. Y. Xue and M. A. Ratner, Phys. Rev. B 69, 85403(2004)

Rupan Preet Kaur, M.Tech from Department of Electronics Technology, G.N.D.U, Amritsar, is doing research in the field of modeling and simulation of electron transport at nanometre scale towards the fabrication of Molecular electronic devices.

Ravinder Singh Sawhney, Professor in the Department of Electronics Technology, Guru Nanak Dev University, Amritsar. He has to his credit more than 40 publications in various international journals as well as international and national conference proceedings.

Published By:
Blue Eyes Intelligence Engineering and Sciences Publication (BEIESP)